JCMS
OPEN ACCESS

www.jclinmedsurgery.com

Journal of
Clinical & Medical Surgery

Research Article

N6-Methyladenosine-Modified Circstat3 Facilitate Tumor Immune Evasion by Targeting PD-L1 in Gastric Cancer

Jinyang Yuan[1]; Wei Lu[2,3]; Chen Wang[3]; Honghong Shen[3]*

[1]Department of General Surgery, The Second Clinical Medical College, Shanxi Medical University, Taiyuan, 030000, People's Republic of China.

[2]Department of Pathology, School of Basic Medicine, Shanxi Medical University, Taiyuan, 030001, People's Republic of China.

[3]Department of pathology, The Second Clinical Medical College, Shanxi Medical University, 382 Wuyi Road, Taiyuan, 030001, People's Republic of China.

***Corresponding Author: Honghong Shen**

The Second Clinical Medical College, Shanxi Medical University, 382 Wuyi Road, Taiyuan, 030001, People's Republic of China.

Tel: +86-3365572; Email: 825267098@qq.com

Article Info

Received: Nov 07, 2022

Accepted: Dec 08, 2022

Published: Dec 19, 2022

Archived: www.jclinmedsurgery.com

Abstract...

Background: An thorough comprehension of immune evasion mechanisms in gastric cancer is crucial to innovate advances in immunotherapy. This study intends to uncover the potential mechanism of N6-methyladenosine-modified circSTAT3 facilitate tumor immune evasion in Gastric Cancer (GC).

Methods: Bioinformatics analysis was performed to identify the circRNAs in GC. A RNA immunoprecipitation (RIP), luciferase reporter assay and RNA pulldown assays were performed to identify the interactions among circSTAT3, miR-34a-3p, miR-34a-3p and PD-L1. The CCK8 assay, FACS, qRT-PCR, western blot and transwell assays were used to investigate the functional roles of circSTAT3 and its downstream target PD-L1 in antitumor immunity in GC. EpiQuiK m6A quantitative kit was used to detect the modification level of m6A in gastric cells.

Results: In the study, we found that circSTAT3 was overexpressed in GC tissues. Functionally, circSTAT3 knockdown could inhibit the GC growth both in vitro and in vivo. Mechanically, circSTAT3 competitively upregulates inflammasome NLRP3 expression by sponging miR-34a-3p. Besides, luciferase reporter assay showed that miR-34a-3p overexpression repressed the luciferase activity of PD-L1-WT, while PD-L1-mut was not affected. ALKBH5 mediates the m6A modification of circSTAT3.

Conclusion: We determined that high circSTAT3 expression is due to enhanced circularization resulting from increased m6A levels of the circSTAT3 transcript in a ALKBH5-dependent manner. This work suggest that circSTAT3/miR-34a-3p/PD-L1 may be a novel therapeutic target in GC treatment and provides a rationale to enhance the efficacy of anti-PD-1 treatment in GC.

Keywords: Gastric cancer; CircSTAT3; miR-34a-3p; m6A; PD-L1

Citation: Yuan J, Lu W, Wang C, Shen H. N6-Methyladenosine-Modified Circstat3 Facilitate Tumor Immune Evasion by Targeting PD-L1 in Gastric Cancer. J Clin Med Surgery. 2022; 2(2): 1062.

Background

Gastric Cancer (GC) is an aggressive disease that is still a global health problem with its heterogeneous nature. In the last several decades, the decrease of gastric cancer incidence has been noted, however it is still the fourth leading cause of cancer-related death worldwide [1]. Researchers worldwide have completed many genomics, transcriptomics, proteomics, and epidemiological investigations and clinical trials regarding the pathogenesis and therapies of gastric cancer [2].

Recently, circular RNAs (circRNAs) are a class of non-coding RNAs characterized by covalently closed continuous loops with neither 5' to 3' polarity nor a polyadenylated tail [3,4]. Accumulating evidence has confirmed the roles of circRNAs in regulating the proliferation, metastasis, stemness and resistance to therapy of GC [5-7]. For example, circFN1 may act as oncogenic circRNA in GC [8]. circRHOBTB3 might function as ceRNA for miR-654-3p, which could contribute to growth inhibition of GC through activating p21 signaling pathway [9]. circNRIP1 sponges miR-149-5p to affect the autophagy associated AKT/mTOR axis and eventually acts as a tumour promotor in GC [10]. However, the biological implications of circRNAs in regulating antitumor immunity in GC remain unclear. Some scholars used bioinformatics analysis method to collect and integrate these circRNAs and summarize them into 6 circRNA database [11-13].

N6-methyladenosine (m6A) is recognized as an abundant co-transcriptional modifification in mRNAs and non coding RNAs (ncRNAs)[14],including circRNAs [15]. Importantly, dysregulated m6A profiles have been implicated in the carcinogenesis and progression of GC. METTL3, the critical methyltransferase of RNA m6A modification, is elevated in GC and induces metastasis in GC cells by enhancing EMT and metastasis in GC [16]. ALKBH5 promotes GC invasion and metastasis by demethylating the lncRNA NEAT1 [17].

Programmed cell death ligand 1 (PD-L1) expression is observed in many malignant tumors and is associated with poor prognosis including gastric cancer (GC). Recent studies have shown that anti-PD-L1/PD-1 antibodies could block tumor progression [18]. A study reported that exosomal PD-L1 predicts the worse survival and reflects the immune status in GC patients [19]. Emerging evidence revealed m6A-marked mRNAs could be a therapeutic target for immunotherapy in combination with emerging checkpoint inhibitors or vaccines [20]. However, the role of m6A-modified circRNAs in regulating the antitumor immunity of GC remain elusive.

The aim of this study was to explore the effect of the circSTAT3/miR-34a-3p axis on PD-L1 expression and its impact on tumor growth and antitumor immunity in vitro and in vivo and to unveil the underlying mechanism of immune escape in GC and identifies a promising new pharmaceutical intervention target for GC patients receiving anti-PD-1 treatment.

Methods

Patients and tissue specimens

Forty-five pairs of GC tissues and adjacent normal tissues were obtained from The Second Affiliated Hospital of Shanxi Medical University. This study was approved by the ethics committee of The Second Affiliated Hospital of Shanxi Medical University. Informed consent was obtained from all patients. All tissues received no radiotherapy or chemotherapy before surgery and immediately frozen at -80°C until use.

Cell culture and transfection

GC cell lines MKN45, MGC-803, HGC-27, BGC-823, SGC-7901 and AGS cells were cultured in DMEM with 10% fetal bovine serum (Gibco, NY, USA). All of the cell lines were purchased from the Chinese Academy of Sciences (Shanghai, China).

The siRNAs targeting circSTAT3 (si-circSTAT3) were synthesized and purchased from GenePharma (Shanghai, China). Scramble siRNA was taken as control. The sequence of circSTAT3 was amplified and cloned into circRNA overexpression vector (circSTAT3) (Geneseed). siRNAs and circSTAT3 (50 nM) were transfected into GC cells using Lipofectamine 3000 (Invitrogen) following the manufacturer's instructions.

RNA extraction and quantitative real-time PCR (qRT-PCR)

Total RNA from the tissue samples or cells was isolated using the Trizol reagent (Invitrogen, Carlsbad, CA, USA) according to the manufacturers instructions. All primers acquired from Sangon Biotech (Shanghai, China). GAPDH or β-actin works as internal control.

Western blotting

Both cells and culture supernatants were harvested for western blotting. The total protein concentration was measured by BCA protein assay kit (P0011, Beyotime) and then separated by SDS-PAGE and transferred to PVDF membranes followed by blocking. The membrane was then incubated overnight with primary antibody against indicated proteins, followed by incubated with HRP-conjugated secondary antibodies. All proteins were visualized with the Tanon High-sig ECL Western Blotting substrate.

RNase R treatment of total RNA

A 2 μg sample of total RNA was treated with 3 U/μg of Rnase R (Epicentre Biotechnologies, cat. no. RNR07250) or water as a control (Mock) for 20 min at 37°C. Digested RNA was subsequently purified using an RNeasy MinElute Cleanup Kit (Qiagen, cat. no. 74204).

Cell viability assay

Cell proliferation capacity was evaluated using the Cell Counting kit-8 (CCK-8; Dojindo Molecular Technologies, Inc., Kumamoto, Japan) according to the manufacturer's protocol. GC cells we reseeded in 96-well plate at density of 1×10^3 per well. Then CCK8 solution were added and absorbance at 450 nm.

Apoptosis assay

Cell apoptosis were measured using an Annexin V-FITC Apoptosis Staining/Detection kit (Cambridge, MA) according to the manufacturer's instructions. FACS was performed to detect the peak of apoptosis cells which showed more ration of intensity.

Trans well assay

Cell migration and invasion was analyzed using the transwell chamber. GC cells (5×10^4) in 200 μL of serum-free medium

were added to the upper chamber coated with or without 50 µL Matrigel for 24 h. The lower chamber was added with medium containing 10% FBS. After incubation, the cells in the upper chamber were removed. And cells in the down chamber were fixed and stained with 0.5% crystal violet (Sigma) and counted.

RNA-Pull down assay

Biotin-labeled circSTAT3 probe was synthesized by Sangon Biotech. circSTAT3-overexpressing GC cells were fixed by 1% formaldehyde for 10 minutes, lysed, and sonicated. After centrifugation, 50 µL of the supernatant was retained as input and the remaining part was incubated with a circSTAT3-specific probesstreptavidin dynabeads (Invitrogen) mixture overnight at 30°C. On the next day, a dynabeads-probes-circRNAs mixture was washed and incubated with 200 µL oflysis buffer and proteinase K to reverse the formaldehyde cross-linking. Finally, the mixture was added with TRIzol for RNA extraction and detection.

Dual-luciferase assay

The putative binding sites of miR-34a-3p and circSTAT3 were subcloned into pmirGLO luciferase promoter plasmid (Promega, Madison, WI, USA). SGC-7901 cells were transfected with luciferase reporter vector and miR-34a-3p using Lipofectamine 3000 (Invitrogen). Luciferase and Renilla signal was measured 48 h after transfection using the Dual-Luciferase Reporter Assay System (Promega).

In vivo xenograft experiments

Xenograft assay was used to analyze the role of circSTAT3 in vivo. 1×10^7 si-circSTAT3 or control cells were subcutaneously injected into the flanks of nude mice from Charles River (Beijing, China). Approximately 5 days later, tumors were detectable and tumor size was measured using a vernier caliper. Tumor volumes were analyzed.

Statistical analysis

Each result from at least three independent experiments was displayed as mean ± standard deviation (SD). All statistical data were analyzed using SPSS software (version 22.0). Statistical significance was measured using Student's t-test. The correlations between expression levels of circSTAT3 and clinicopathological features of GC patients were analyzed by Chi-square test. $P<0.05$ was considered to be statistically significant.

Results

circSTAT3 is upregulated in GC

Firstly, in order to investigate the relationship between circRNA and GC, we analyzed the online GEO dataset (GSE43633). According to this data, we found that circSTAT3 is the most upregulated circRNA in GC tissues compared to adjacent normal control tissues (Figure 1A). Thus, we chose it to further investigation. Subsequently, circSTAT3 expression in 6 GC cell lines were checked, including MKN45, MGC-803, HGC-27, BGC-823, SGC-7901 and AGS cells. Our findings suggested that SGC-7901 and AGS cells had higher circSTAT3 expression levels, while MGC-803 and BGC-823 cells had expressed lower levels of circSTAT3 (Figure 1B). As shown, the expression of circSTAT3 was markedly upregulated in collected 45 GC tissues compared to their corresponding adjacent normal tissues (Figure 1C). Besides, as to analyze the correlation between circSTAT3 expression and clinicopathological features of GC patients, patients were further classified into two groups, namely, the low-level and high-level groups, based on the median value of circSTAT3 expression in GC tissues. As shown in Table, patients with higher circSTAT3 expression level were associated with a larger tumor, higher TNM stage and lymph node metastasis than those with low circSTAT3 expression level. Meanwhile, the relationship between circSTAT3 expression and the prognosis for GC patients were also analyzed. The Kaplan-Meier survival curves demonstrated that GC patients with higher circSTAT3 expression level had a shorter Overall Survival (OS) rate than that in the low-level group (Figure 1D). Moreover, ROC analysis showed that circSTAT3 was reliable biomarkers for differentiating GC from normal controls with AUC of 0.766 (Figure 1E, specificity: 66.86%, sensitivity: 81.32%). These results suggested that upregulation of circSTAT3 might serve as an oncogene for GC progression.

Figure 1: The correction between circSTAT3 and clinicopathological feature of gastric cancer patients.

Characteristics		circPTK2		*P*-value
		Low N %	High N %	
All	45	15 33.3	30 66.7	
Age				
≤55	17	6 35.3	11 64.7	0.984
>55	28	9 32.1	19 67.9	
Gender				
Male	37	12 32.4	25 67.6	0.783
Female	18	5 27.8	13 72.2	
Tumor size (cm)				
<5	17	9 52.9	8 47.1	0.008*
≥5	38	6 15.8	32 84.2	
Degree of differentiation				
Well differentiated	4	2 50.0	2 50.0	0.557
Moderately differentiated	18	6 33.3	12 66.7	
Poorly differentiated	23	8 34.8	15 65.2	
TNM stage				
Stage I	11	6 54.5	5 45.5	0.036*
Stage II	10	4 40.0	6 60.0	
Stage III	16	6 37.5	10 62.5	
Stage IV	8	2 25.0	6 75.0	
LNs metastasis				
No	20	9 45.0	11 55.0	0.030*
Yes	25	6 24.0	19 76.0	
Distant metastasis				
No	40	13 32.5	27 67.5	0.830
Yes	5	2 40.0	3 60.0	
CEA				
Negative	32	10 31.2	22 68.8	0.851
Positive	13	4 30.8	9 69.2	
CA12-5				
Negative	31	10 32.2	21 67.8	0.883
Positive	14	5 35.7	9 64.3	
CA19-9				
Negative	35	11 31.4	24 68.6	0.901
Positive	10	3 30.0	7 70.0	

A

Bioinformatics analysis of differentially expressed circRNAs in gastric cancer

No.	circRNA ID	Fold Change	Regulation	Chrom	Gene symbol
1	hsa_circ_0121787	-4.008525827	down	chr3	RAF1
2	hsa_circ_0039992	-3.130155951	down	chr16	CDH1
3	hsa_circ_0060300	5.987219938	up	chr20	STAT3
4	hsa_circ_0136265	5.352111874	up	chr8	EXTL3
5	hsa_circ_0096363	4.861786326	up	chr11	PTK2
6	hsa_circ_0052535	4.554621882	up	chr2	ASAP2
7	hsa_circ_0006477	4.27229782	up	chr5	RASA1
8	hsa_circ_0062525	4.086742493	up	chr22	BCR
9	hsa_circ_0031836	4.034723427	up	chr14	SOS2
10	hsa_circ_0067047	3.961119931	up	chr3	MYLK
11	hsa_circ_0027118	3.716896041	up	chr12	STAT6
12	hsa_circ_0007880	3.428142649	up	chr8	SHANK2

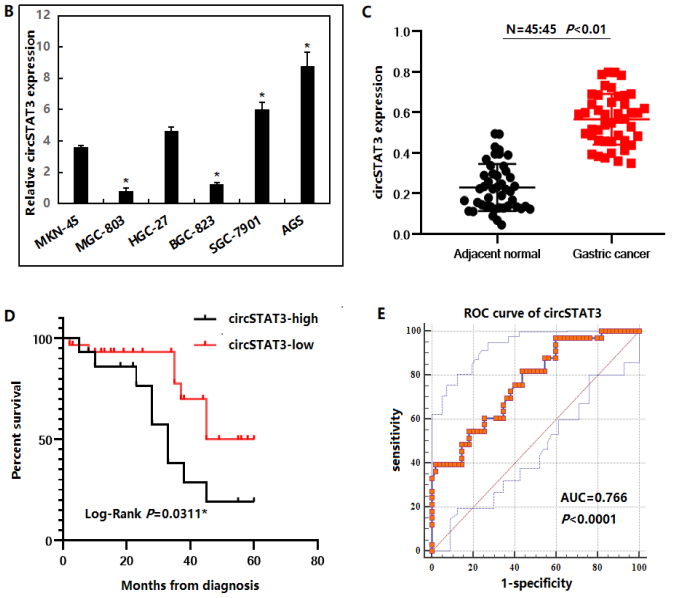

Figure 1: circSTAT3 is upregulated in GC. (**A**) According to a public dataset (GSE43633), circSTAT3 expression was upregulated in GC tissues. (**B**) The circSTAT3 expression levels in different GC cell lines were examined by qRT-PCR. (**C**) The circSTAT3 expression levels in 45 pairs of GC and adjacent normal tissues were detected by qRT-PCR. (**D**) The prognosis of GC patients with different expression level of circSTAT3 was examined by Kaplan-Meier curves and logrank test. (**E**) ROC analysis for distinguishing GC cases from controls using circSTAT3. *P<0.05.

The characteristic of cirSTAT3

Subsequently, total RNA was treated with RNase R to analyze the stability of circSTAT3. As expected, circSTAT3 showed higher resistance to RNase R digestion, compared to the linear mRNA control (Figure 2A). Moreover, the circSTAT3 transcript exhibited a half-life >24h after treatment with actinomycin D, while its linear counterpart showed a half-life<6h (Figure 2B). These analyses provided additional support that circSTAT3 has stable circRNA structure. Since recent reports have proposed that the function of circRNAs is associated with their subcellular compartmentalization, circSTAT3 localization was addressed by Fluorescence *In Situ* Hybridization (FISH), which directly revealed a clear cytoplasmic localization (Figure 2C); nuclear/cytoplasmic fractionation was performed on GC cells to determine circSTAT3 localization. qRT-PCR analysis confirmed that circSTAT3 was enriched in the cytoplasmic fraction (Figure 2D). Altogether, these results demonstrate that circSTAT3 is an highly stable circRNA present in the cytoplasm of GCs. Subsequently, circSTAT3 siRNA was transfected into SGC-7901 and AGS cells, and the knockdown efficiencies were detected using qRT-PCR (Figure 2E). Moreover, circRNA overexpression plasmid was co-transfected with the circular frame into MGC-803 and BGC-823 cells, the results of which demonstrated that circSTAT3 could be evidently upregulated in these two GC cell lines (Figure 2F).

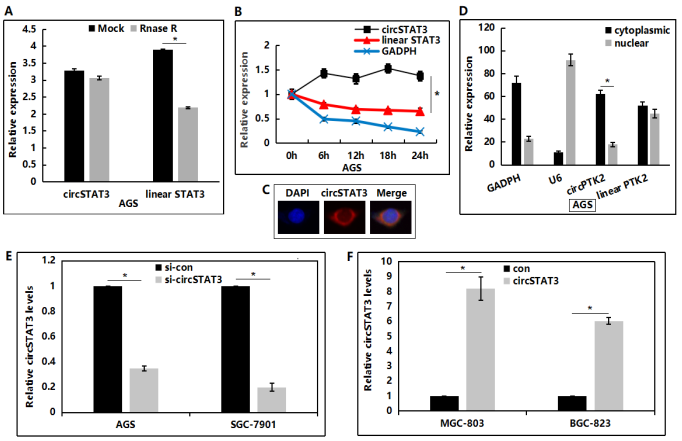

Figure 2: The characteristic of cirSTAT3. (**A**) qRT-PCR was used to measure the abundance of circSTAT3 and linear STAT3 mRNA after RNase R treatment. (**B**) qRT-PCR was used to determine the abundance of circSTAT3 and linear STAT3 mRNA in GC cell treated with actinomycin D at the indicated time points. (**C**) The FISH assay showed the localization of circSTAT3, with 4,6-diamidino-2-phenylindole (DAPI), used to stain the cell nuclei. (**D**) Cytoplasmic and nuclear fractions of cellular RNA were analyzed for circSTAT3 expression by qRT-PCR and expressed as a percentage of the input. U6 and GAPDH mRNA were used as reference RNAs for nuclear and cytoplasmic fractions, respectively. (**E**) The relative expression of circSTAT3 was detected using qRT-PCR following transfection with si-con or si-circSTAT3 in AGS and SGC-7901 cells. (**F**) The relative expression of circSTAT3 was detected using qRT-PCR following transfection with empty vector or overexpressed circSTAT3 plasmid in MGC-803 and BGC-823 cells.

cirSTAT3 promotes the proliferation, invation while inhibits the apoptosis and pyroptosis of GC cells *in vitro*

CCK-8 assays showed that depletion of circSTAT3 could dramatically suppress the proliferation of AGS (Figure 3A) and SGC-7901 cells (Figure 3B). In contrast, overexpression of circSTAT3 would enhance the proliferative capacity of both MGC-803 (Figure 3C) and BGC-823 cells (Figure 3D). Afterwards, FACS analysis was also performed to detect the effect of circSTAT3 on the apoptosis of GC cells. Our findings revealed that, compared with the control cells, the circSTAT3-silencing AGS and SGC-7901 cells had notably higher percentages of Annexin V-positive cells (Figure 3E), whereas circSTAT3 overexpression would inhibit cell apoptosis (Figure 3F). The expression of pyroptosis protein markers, NLRP3, caspase-11 and GSDMD was upregulated in the circSTAT3-silencing AGS cells (Figure 3G) and dowenregulated in the circSTAT3 overexpression MGC-803 cells (Figure 3H). Additional western blot demonstrated the significantly increased levels of TGF-βin si-circSTAT3 group (Figure 3G), whereas circSTAT3 overexpression decreased the expression levels of TGF-β (Figure 3H). Transwell assay were then used to explore the effects of circSTAT3 on the invasion of GC cells. The results supported that, circSTAT3 knockdown could suppress the invasion of AGS and SGC-7901 cells (Figure 3I). The invasive capacities of MGC-803 and BGC-823 cells were markedly promoted after the overexpression of circSTAT3 (Figure 3J).

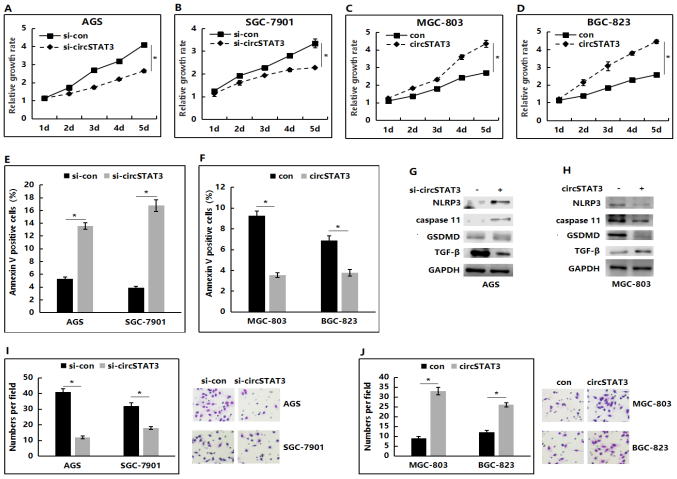

Figure 3: cirSTAT3 promotes the proliferation, invasive while inhibits the apoptosis and pyroptosis of GC cells in vitro. (**A and B**) The effect of cirSTAT3 knockdown on the proliferation of AGS and SGC-7901 cells was detected by CCK-8 assay. (**C and D**) The effect of cirSTAT3 overexpression on the proliferation of MGC-803 and BGC-823 cells was detected by CCK-8 assay. (**E**) cirSTAT3 knockdown increased apoptotic GC cells. (**F**) cirSTAT3 overexpression decreased apoptotic GC cells. (**G and H**) Western blot was performed to detect the pyroptosis markers in GC cells with cirSTAT3 knockdown(**G**)or overexpression(**H**). (**I and J**) Western blot was performed to detect the autophagy markers in GC cells with cirSTAT3 knockdown(**I**)or overexpression(**J**). (**K**) A transwell assay was used to measure the invasion ability after knockdown of circSTAT3 in AGS and SGC-7901 cells. (**L**) A transwell assay was used to measure the invasion ability after overexpression of circSTAT3 in MGC-803 and BGC-823 cells.

cirSTAT3 associates with miR-34a-3p

circRNA is found to serve as a miRNA sponge to regulate miRNA targets. Through CircInteractome prediction (https://circinteractome.nia.nih.gov/), 5 miRNAs were predicated as the potential targets of circSTAT3 (Figure 4A). Interestingly, results of RNA-Pull down assay indicated a specific enrichment of circSTAT3 and miR-34a-3p compared with the controls, whereas the other miRNAs were not enriched (Figure 4B). Afterwards, the potential binding site between circSTAT3 and miR-34a-3p as well as its mutant type was constructed based on CircInteractome prediction (Figure 4C). SGC-7901 cells were co-transfected with miR-34a-3p and a luciferase reporter containing the full length of circSTAT3 3′-UTR (wild-type) or a mutant. Luciferase intensity was measured after 48 hours for transfection. miR-34a-3p markedly decreased the luciferase intensity in luciferase wild-type reporter construct (Figure 4D). To determine whether circSTAT3 was regulated by miR-34a-3p in AGO2-dependent manner, anti-AGO2 RNA immunoprecipitation was conducted, the results showed that circSTAT3 pull-down by AGO2 was specifically enriched in SGC-7901 cells transfected with miR-34a-3p mimics (Figure 4E), indicating that miR-34a-3p was a circSTAT3-targeting miRNA. Moreover, depletion of circSTAT3 could lead to increased miR-34a-3p expression (Figure 4F), while ectopic circSTAT3 expression would downregulate miR-34a-3p transcription (Figure 4G).

A

The circSTAT3 downstream miRNA

ID	Family	MSA Start	MSA End	Site Type
1	miR-2117	90	97	8mer-1a
2	miR-3065-3p	82	88	7mer-1a
3	miR-3120-3p	24	30	7mer-1a
4	miR-3127-5p	50	56	7mer-1a
5	miR-34a-3p	41	48	8mer-1a

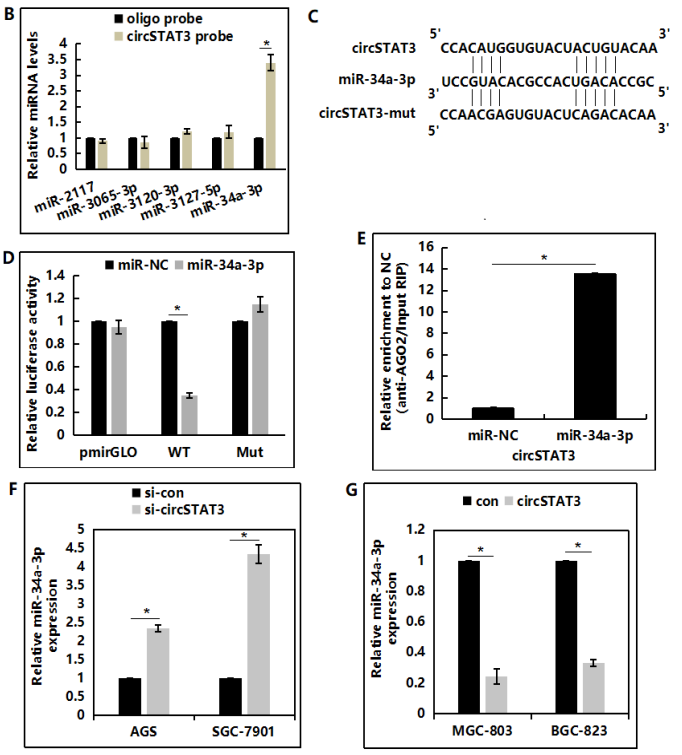

Figure 4: cirSTAT3 associates with miR-34a-3p. (**A**) Through CircInteractome prediction predicated potential targets miRNAs of circSTAT3. (**B**) The endogenous miRNAs assoicated with circSTAT3 was examined by RNA-Pull down assay. (**C**) The mutative sequences of miR-34a-3p and with 9 paired nucleotides. (**D**) Luciferase activity in SGC-7901 cells cotransfected with miR-34a-3p and luciferase reporters containing wild-type (WT) and mutant circSTAT3 (Mut) transcript. (**E**) The amout of circSTAT3 pulled down by AGO2 antibody was detected by RIP assay after miR-34a-3p transfection. (**F**) The miR-34a-3p expression was determined by qRT-PCR in AGS and SGC-7901 cells with circSTAT3 knockdown. (**G**) The miR-34a-3p expression was determined by qRT-PCR in MGC-803 and BGC-823 cells with circSTAT3 overexpression.

circSTAT3 functions through suppressing miR-34a-3p

miR-34a-3p expression in GC cell lines were checked. Our findings suggested that SGC-7901 and AGS cells had lower miR-34a-3p expression levels, while MGC-803 and BGC-823 cells had expressed higher levels of miR-34a-3p (Figure 5A). As shown, the expression of miR-34a-3p was markedly deregulated in collected 18 GC tissues compared to their corresponding adjacent normal tissues (Figure 5B). Because previous experiments had verified that circSTAT3 promoted the tumorigenicity of gastric cell lines and circSTAT3 acted as an miR-34a-3p sponge, we performed the rescue experiments to assess whether miR-34a-3p was involved in the circSTAT3-induced malignant phenotypes. Our results indicated that miR-34a-3p inhibitor could abrogate the effect of circSTAT3 on suppressing the proliferation and invasion of SGC-7901 cells (Figure 5C and 5D). Conversely, the overexpression of miR-34a-3p could also reverse the elevated proliferation and invasion induced by the overexpression of circSTAT3 (Figure 5E and 5F).

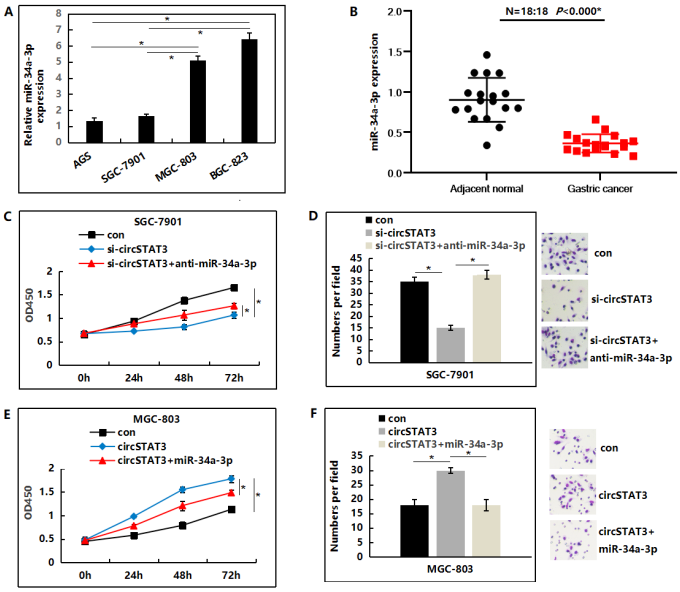

Figure 5: circSTAT3 functions through suppressing miR-34a-3p. (**A**)The miR-34a-3p expression levels in different GC cell lines were examined by qRT-PCR. (**B**) The miR-34a-3p expression levels in 18 pairs of GC and adjacent normal tissues were detected by qRT-PCR. (**C and D**) The miR-34a-3p inhibitor resuced the decrease of proliferation (**C**) and invasion (**D**) mediated by circSTAT3 knockdown in SGC-7901 cells. (**E and F**) The miR-34a-3p overexpression abolished the proliferation (**E**) and invasion (**F**) enhanced by circSTAT3 overexpression in MGC-803 cells. *P<0.05.

miR-34a-3p regulates PD-L1 expression at the post-transcriptional level

We have previously confirmed that circSTAT3 inhibits the pyroptosis of gastric cancer cells, and further bioinformation prediction suggested that PD-L1 was one of the target genes of miR-34a-3p (Figure 6A). The expression level of PD-L1 was obviously higher in gastric cancer tissues than in normal adjacent tissues (Figure 6B). In view of the results, we wondered whether miR-34a-3p directly targeted PD-L1. To verify the hypothesis, we cloned the predicted binding sequence of PD-L1's 3'UTR into the luciferase reporter plasmid to explore the miR-34a-3p's targets specifcity. The results were shown in Figure 6C,D. The relative luciferase activity of the wild-type 3'-UTR was signifcantly repressed following miR-34a-3p mimic transfection compared to control in AGS cells whereas the mutant not. We next validated our findings in clinical samples. IHC staining showed that TGF-βexpression was positively correlated with PD-L1 expression (Figure 6E).

ALKBH5 mediated circSTAT3 in gastric cancer

CircScan analysis was used to predict the protein bound to circSTAT3, in which ALKBH5 was the key catalytic enzyme modified by m6A (Figure 6F). In order to further explore the upstream mechanism of circSTAT3 regulating the occurrence and development of gastric cancer, we further extracted total RNAs from the four GC cells and used EpiQuiK m6A quantitative kit to detect the modification level of m6A. The results showed that the m6A modification level in circSTAT3 cells with high expression showed a downregulation trend compared with circSTAT3 cells with low expression (P<0.05) (Figure 6G), suggesting that the decrease of m6A modification level may be related to the occurrence and development of GC. Consistently, the ALKBH5 mRNA expression was down-regulated both in MGC803 and BGS823 gastric cancer cell lines (Figure 6H).

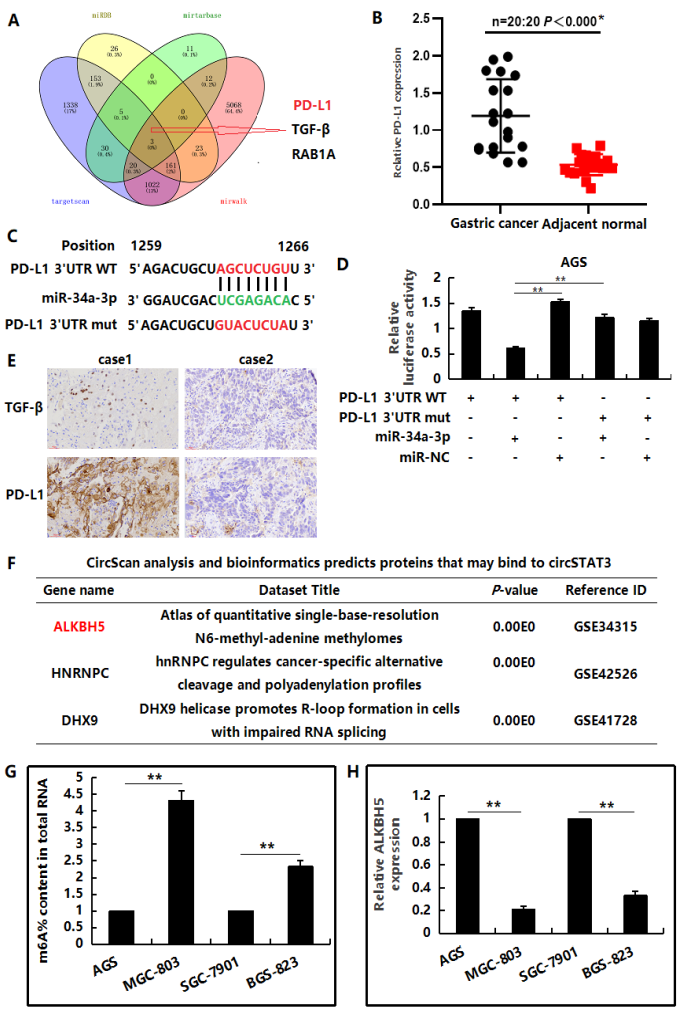

Figure 6: (**A**) Bioinformatics prediction of miR-34a-3p downstream target genes. (**B**) The expression level of PD-L1 was upregulated in gastric cancer samples (n=20), as determined by qRT-PCR. (**C**) Bioinformatics predicated binding sequence between miR-34a-3p and PD-L1. (**D**) Luciferase reporter assay showed that miR-34a-3p overexpression signifcantly repressed the luciferase activity of PD-L1-wt, while the luciferase activity of PD-L1-mut was not afected in AGS cells. (**E**) Representative images of IHC staining of TGF-βand PD-L1 in two GC samples from cohort. (**F**) CircScan analysis and bioinformatics prediction of potential circSTAT3 binding proteins. (**G**) m6A quantitative kit was used to detect the m6A modification level in GC cells. (**H**) The expression of ALKBH5 in gastric cancer cell lines was determined by qRT-PCR.

cirSTAT3 facilitates the growth and pyroptosis of GC cells in vivo

Furthermore, xenograft assay was used to test the effect of circSTAT3 on GC in vivo. As shown, circSTAT3 knockdown significantly suppressed the tumor size at described time points (Figure 7A). At the endpoint, tumor weights were measured. Results showed that circSTAT3 silencing also markedly decreased the tumor weights (Figure 7B). Morever, IHC suggested that downregulation of circSTAT3 in SGC-7901 cells would lead to reduced the expression of GSDMD and PD-L1 in tumor tissue (Figure 7C). Conversely, overexpression of circSTAT3 could significantly promote tumor growth (Figure 7D and E) and increased the expression of GSDMD and PD-L1 (Figure7F) in MGC-803 cells in vivo. Taken together, our results illustrated the important role of the circSTAT3/miR-34a-3p/PD-L1 axis in gastric cancer cell escape from immune surveillance (Figure7G).

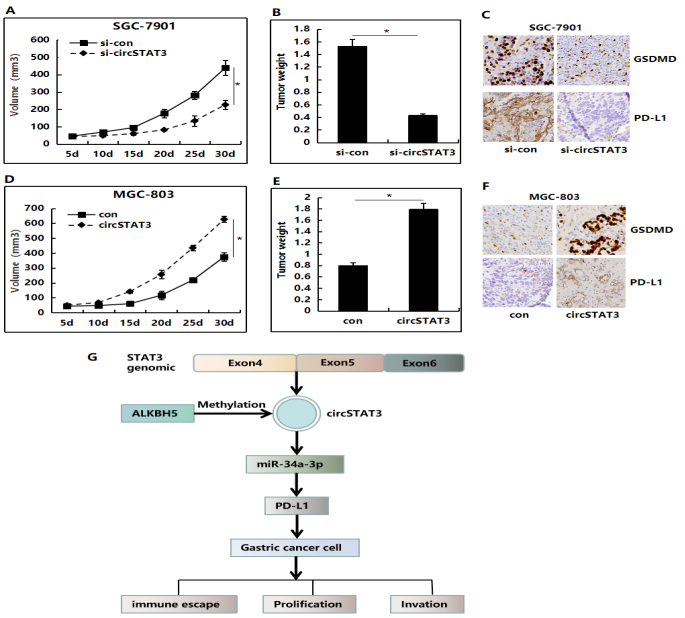

Figure 7: cirSTAT3 facilitates the growth, while inhibits the pyroptosis of GC cells in vivo. (**A and B**) SGC-7901 cells stably expressing circSTAT3 siRNA or the negative control were used for in vivo tumorigenesis. The tumor volumes were measured every 5 days after inoculation (**A**). Tumor weights are represented (**B**). (**C**) Images showing representative IHC staining of GSDMD and PD-L1 in tumor tissue samples from the SGC-7901 cells stably expressing circSTAT3 siRNA or the negative control. (**D and E**) MGC-803 cells stably expressing circSTAT3 or the control were used for in vivo tumorigenesis. (**F**) Images showing representative IHC staining of GSDMD and PD-L1 in tumor tissue samples from the MGC-803 cells stably expressing circSTAT3 or control. (**G**) Schematic representation of the oncogenesis effect of the circSTAT3.

Discussion

Gastric cancer is one of the most common malignancies worldwide; it has the second highest incidence and mortality rate of all cancers. Although the exact cause of gastric cancer is unclear, its pathogenesis is the same as that of other malignant tumors: it is a multi-step, multi-factorial comprehensive disease [21,22]. Previous studies have shown differentially expressed circRNAs between GC and matched normal gastric tissues through RNA sequencing or chip microarray [23-25]. In our study, a novel circRNA, circSTAT3, was shown to be aberrantly expressed in GC, and that circSTAT3 was significantly upregulated in GC tissues and cell lines. Gain-of-function and loss-of-function experiments demonstrated that circSTAT3 was associated with proliferation, invation and pyroptosis of GC cells in vitro and in vivo, suggesting that circSTAT3 acts as a tumor promoter role in gastric cancer. These fndings prompted us to explore the regulatory mechanism of circSTAT3 in GC.

It has been acknowledged that circRNAs primarily function as miRNA sponges to competitively upregulate the expression of miRNA targeted genes [26]. miR-34a-3p has been shown an independent biomarker associated with a lower risk of recurrence in Non-muscle-invasive bladder cancer [27]. On the other hand, deregulation of miR-34a-3p alters proliferation and apoptosis by targeting SMAD4, FRAT1 and BCL2 of meningioma cells [28]. However, no reports are available regarding the association between circRNAs and miR-34a-3p so far. In our study, we performed bioinformatic analyses to select miRNAs, which shared common binding sites of circSTAT3 and miR-34a-3p. Simultaneously, we designed circSTAT3 luciferase reporter screening for these miRNAs. We found that miR-34a-3p reduced the luciferase activity of circSTAT3 luciferase reporter most. Considering the strongest binding strength with circSTAT3, miR-34a-3p was verified as the binding target of circSTAT3, suggesting that circSTAT3 may function as a ceRNA by competitively bound to miR-34a-3p.

As we all known, microRNAs are involved in tumorigenesis by regulating the expression of target genes. In our study, we found that TGF-βand PD-L1 are the targets of miR-34a-3p in gastric cancer cells by bioinformatics analysis and luciferase reporter assay. PD-L1 has been speculated to play a major role in suppressing the immune system that allows immune escape of tumor cells [29]. It has been proven that PD-L1 can be regulated at both the transcriptional and post transcriptional levels [30]. Thus, to further reveal the potential regulatory mechanisms under these genomic loci, studies on the pathological functions of small noncoding RNAs are required. Our study found that miR-34a-3p could inhibit PD-L1 expression by binding to its mRNA 3'UTR, which was at the transcription level. Thus, miR-34a-3p likely elicits tumor suppressive efects through the regulation of PD-L1 expression. The novel mechanism that miR-34a-3p regulates PD-L1 expression may shed light on the immune checkpoint inhibitor therapy in GC.

Although m6A modification has been reported as widespread in circRNAs and can be recognized by YTHDF1 and YTHDF2, m6A-modified circRNAs exhibit less stability when regulated by YTHDF2 [31]. On the other hand, ALKBH5 is shown to mediating export and metabolism of m6A-modified mRNAs [32]. Additionally, ALKBH5 can regulate metabolite/cytokine content and filtration of immune cells in tumor microenvironment during anti-PD-1 therapy [33]. We identified that circSTAT3 is interacted with ALKBH5 from mass spectrometry. To our knowledge, this is the first report to provide insight into the regulatory mechanism of m6A modification-mediated circRNA in GC. Here, we demonstrated that m6A modification level in circSTAT3 cells with high expression showed a downregulation trend compared with circSTAT3 cells with low expression, and ALKBH5 mRNA level in circSTAT3 cells with high expression showed a upregulation trend compared with circSTAT3 cells with low expression, suggesting that the ALKBH5 exhibits a important function in promoting m6A-modified circSTAT3 exert their biological functions. In GC, ALKBH5 promotes GC invasion and metastasis by demethylating the lncRNA NEAT1 [34]. However, little is known about whether m6A modification-mediated circRNA participates in tumor immunity in GC.

Conclusion

In conclusion, our study not only dissected the molecular mechanism of circSTAT3 upregulation but also revealed a novel immunosuppressive effect of PD-L1 in GC. Our findings reveal that circSTAT3 relieves the inhibitory effect of miR-34a-3p by acting as an miRNA sponge and that stabilizes PD-L1 at transcriptional level and post-transcriptional level. At the same time, our results supports an emerging paradigm of m6A as a potential selective signal for the metabolism of circular RNAs. Our study indicates that circSTAT3 might be considered as a prognosis marker of GC and PD-L1 acts as a potential therapeutic target in the management of GC.

Declarations

Ethical approval: This study was approved by the Second Clinical Medical College, Shanxi Medical University, China and has been performed in accordance with the ethical standards

laid down in the 1964 Helsinki declaration and its later amendments.

Conflict of interest: The authors declare no conflict of interest.

Informed consent: Informed consent was obtained from all individual patients enrolled in the study.

Abbreviations: 3'-UTR: 3'Untranslated regions; PD-L1: Programmed death-ligand 1; GC: Gastric cancer/carcinoma; GEO: Gene Expression Omnibus; LNs: Lymphy Nodes; siRNA: small interfering RNA; OS: overall survival; FISH: Fluorescence in Situ Hybridization.

References

1. Zhang X, Zhang P. Gastric cancer: Somatic genetics as a guide to therapy. J Med Genet. 2017; 54: 305-312.
2. Sulahian R, Casey F, Shen J, Qian ZR, Shin H, et al. An integrative analysis reveals functional targets of GATA6 transcriptional regulation in gastric cancer. Oncogene. 2014; 33: 5637-5648.
3. Zhao J, Lee EE, Kim J, Yang R, Chamseddin B, et al.Transforming activity of an oncoprotein-encoding circular RNA from human papillomavirus. Nat Commun. 2019; 10: 2300.
4. TToptan T, Abere B, Nalesnik MA, Swerdlow SH, Ranganathan S, et al. Circular DNA tumor viruses make circular RNAs.Proc Natl Acad Sci U S A. 2018; 115: E8737-E8745.
5. Li X, Yang L, Chen LL The biogenesis, functions, and challenges of circular RNAs. Mol Cell. 2018; 71: 428-442.
6. Mihnea Dragomir, George A. Calin.Circular RNAs in Cancer- Lessons Learned From microRNAs. Front Oncol. 2018; 8: 307.
7. Alexander Wesselhoeft R, Piotr S. Kowalski, Daniel G. Anderson. Engineering circular RNA for potent and stable translation in eukaryotic cells. Nat Commun. 2018; 9: 2629.
8. Huang XX, Zhang Q, Hu H, Jin Y, Zeng AL, et al. A novel circular RNA circFN1 enhances cisplatin resistance in gastric cancer via sponging miR-182-5p. J Cell Biochem. 2020.
9. Deng G, Mou T, He J, Chen D, Lv D, et al. Circular RNA circRHOBTB3 acts as a sponge for miR-654-3p inhibiting gastric cancer growth. J Exp Clin Cancer Res. 2020; 39: 1.
10. Zhang X, Wang S, Wang H, Cao J, Huang X, et al. Circular RNA circNRIP1 acts as a microRNA-149-5p sponge to promote gastric cancer progression via the AKT1/mTOR pathway. Mol Cancer. 2019; 18: 20.
11. Liu YC, Li JR, Sun CH, Andrews E, Chao RF, et al. CircNet: a database of circular RNAs derived from transcriptome sequencing data. Nucleic Acids Res. 2016; 44: D209-D215.
12. Zheng LL, Li JH, Wu J, Sun WJ, Liu S, et al. deepBase v2.0: identification, expression, evolution and function of small RNAs, LncRNAs and circular RNAs from deep-sequencing data. Nucleic Acids Res. 2016; 44: D196-D202.
13. Dawood B. Dudekula, Amaresh C. Panda, Ioannis Grammatikakis, Supriyo De, Kotb Abdelmohsen, Myriam Gorospe. CircInteractome: A web tool for exploring circular RNAs and their interacting proteins and microRNAs. RNA Biol. 2016; 13: 34-42.
14. Gilbert WV, Bell TA, Schaening C. Messenger RNA modifications: Form, distribution, and function. Science. 2016; 352: 1408-1412.
15. Zhou C, Molinie B, Daneshvar K, Pondick JV, Wang J, et al. Genome-wide maps of m6A circRNAs identify widespread and cell-type-specific methylation patterns that are distinct from mRNAs. Cell Rep. 2017; 20: 2262-2276.
16. Yue B, Song C, Yang L, Cui R, Cheng X, et al. METTL3-mediated N6-methyladenosine modification is critical for epithelial-mesenchymal transition and metastasis of gastric cancer.Mol Cancer. 2019; 18:142.
17. Zhang J, Guo S, Piao HY, Wang Y, Wu Y, et al. ALKBH5 promotes invasion and metastasis of gastric cancer by decreasing methylation of the lncRNA NEAT1.J Physiol Biochem. 2019; 75: 379-389.
18. Rittmeyer A, Barlesi F, Waterkamp D, Park K, Ciardiello F, et al. Atezolizumab versus docetaxel in patients with previously treated non-small-cell lung cancer (OAK): a phase 3, open-label, multicentre randomised controlled trial. Lancet. 2017; 389: 255-265.
19. Fan Y, Che X, Qu J, Hou K, Wen T, et al. Exosomal PD-L1 Retains Immunosuppressive Activity and is Associated with Gastric Cancer Prognosis. Ann Surg Oncol. 2019; 26: 3745-3755.
20. Han D, Liu J, Chen C, Dong L, Liu Y, et al. Anti-tumour immunity controlled through mRNA m(6)A methylation and YTHDF1 in dendritic cells. Nature. 2019; 566: 270-274.
21. Abe Y, Hirano H, Shoji H, Tada A, Isoyama J, et al. Comprehensive characterization of the phosphoproteome of gastric cancer from endoscopic biopsy specimens.Theranostics. 2020;10: 2115-2129.
22. Rachel S van der Post, Ingrid P Vogelaar, Fátima Carneiro, Parry Guilford, David Huntsman, et al. Hereditary diffuse gastric cancer: updated clinical guidelines with an emphasis on germline CDH1 mutation carriers. J Med Genet. 2015; 52: 361-374.
23. Lei M, Zheng G, Ning Q, Zheng J, Dong D.Translation and functional roles of circular RNAs in human cancer. Mol Cancer. 2020; 19: 30.
24. Wang S, Tang D, Wang W, Yang Y, Wu X, et al. circLMTK2 acts as a sponge of miR-150-5p and promotes proliferation and metastasis in gastric cancer. Mol Cancer. 2019; 18: 162.
25. Lu J, Wang YH, Yoon C, Huang XY, Xu Y, et al. Circular RNA circRanGAP1 regulates VEGFA expression by targeting miR-877-3p to facilitate gastric cancer invasion and metastasis. Cancer Lett. 2020; 471: 38-48.
26. Salmena L, Poliseno L, Tay Y, Kats L, Pandolfi PP. A ceRNA hypothesis: the Rosetta Stone of a hidden RNA language? Cell. 2011; 146: 353-358.
27. Juracek J, Stanik M, Vesela P, Radova L, Dolezel J, et al.Tumor expression of miR-34a-3p is an independent predictor of recurrence in non-muscle-invasive bladder cancer and promising additional factor to improve predictive value of EORTC nomogram. Urol Oncol. 2019; 37: 184.e1-184.e7.
28. Werner TV, Hart M, Nickels R, Kim YJ, Menger MD, et al. MiR-34a-3p alters proliferation and apoptosis of meningioma cells in vitro and is directly targeting SMAD4, FRAT1 and BCL2.Aging (Albany NY). 2017; 9: 932-954.
29. Mariathasan S, Turley SJ, Nickles D, Castiglioni A, Yuen K, et al. TGFβ attenuates tumour response to PD-L1 blockade by contributing to exclusion of T cells. Nature. 2018; 554: 544-548.
30. Liu H, Kuang X, Zhang Y, Ye Y, Li J, et al. ADORA1 inhibition promotes tumor immune evasion by regulating the ATF3-PD-L1 Axis. Cancer Cell. 2020; 37: 324-39e328.
31. Chan Zhou, Benoit Molinie, Kaveh Daneshvar, Joshua V. Pondick, Jinkai Wang, et al. Genome-wide maps of m6A circRNAs identify widespread and cell-type-specific methylation patterns that are

distinct from mRNAs. Cell Rep. 2017; 20: 2262-2276.

32. Wang J, Wang J, Gu Q, Ma Y, Yang Y, et al. The biological function of m6A demethylase ALKBH5 and its role in human disease. Cancer Cell Int. 2020; 20: 347.

33. Li N, Kang Y, Wang L, Huff S, Tang R, et al. ALKBH5 regulates anti-PD-1 therapy response by modulating lactate and suppressive immune cell accumulation in tumor microenvironment.Proc Natl Acad Sci U S A. 2020; 117: 20159-20170.

34. Zhang J, Guo S, Piao HY, Wang Y, Wu Y, et al. ALKBH5 promotes invasion and metastasis of gastric cancer by decreasing methylation of the lncRNA NEAT1. J Physiol Biochem. 2019; 75: 379-389.